Resonant Magneto-optical Transitions from a Mid-Gap Level in *n*-InSb

D. G. Seiler, M. W. Goodwin, and A. Miller
Department of Physics, North Texas State University, Denton, Texas 76203
(Received 26 November 1979)

The first magneto-optical transitions originating from a deep defect level in high-purity *n*-InSb are observed in the CO_2-laser–induced resonant photoconductivity at low magnetic fields. Another series of resonant structures is associated with three-LO-phonon–assisted spin-conserving cyclotron harmonic transitions.

The large number of magneto-optical experiments on InSb have enhanced our understanding of many of its properties—electronic, lattice, and impurity. In fact, InSb is one of the best-characterized semiconducting materials. In this paper we present some important results on the nonequilibrium electron dynamics in *n*-InSb ($n \simeq 9 \times 10^{13}$ cm^{-3}) induced by a CO_2 laser, which provide new information on the magneto-optical properties of *n*-InSb, in spite of the large number of previous experiments. These studies have been carried out with a photoconductivity technique which has proven capable of detecting weak magneto-optical transitions at low magnetic fields. In this low-field region, the CO_2-laser–induced magnetophotoconductivity exhibits resonant structure which depends upon the photon energy, the laser intensity, the magnetic field, and the lattice temperature. Two distinctly different series of resonant structures are identified as arising from (1) three-LO-phonon cyclotron resonant harmonic (LOCRH) transitions and (2) defect cyclotron resonance harmonic (DCRH) transitions from a *deep defect level*.

Theoretical descriptions of these deep impurity or defect levels are complicated but can have important technological consequences for both electrical and optical devices. However, there have been few attempts to study these levels with magneto-optical techniques. For the first time, magneto-optical transitions from a deep level in *n*-InSb have been identified. This has been possible because of the enhanced signal-to-noise ratio provided by simultaneous use of both sampling oscilloscope and lock-in amplifier techniques that were previously developed by Kahlert and Seiler.[1] A constant dc electrical current of 5 mA is applied to a sample of 0.2×1-mm^2 cross section while an ac magnetic field of 150 G modulates the sample conductivity at a frequency of 43 Hz. The photoconductive signal produced by the laser pulse (~10 μsec wide from a mechanically chopped focused laser beam with a 3% duty cycle to eliminate lattice heating) is fed to a Tektronix model 7904/7S14 sampling oscilloscope. The output of the 7S14 is then fed into a lock-in amplifier tuned to 86 Hz which results in a lock-in detector response proportional to the second derivative of the photoconductive signal.

Figure 1 shows reproductions of the output of the lock-in detector versus inverse magnetic field for various relative peak incident laser powers at 9.56 μm. The laser power was attenuated with calibrated filters and an absorption cell filled with propylene of variable pressures.

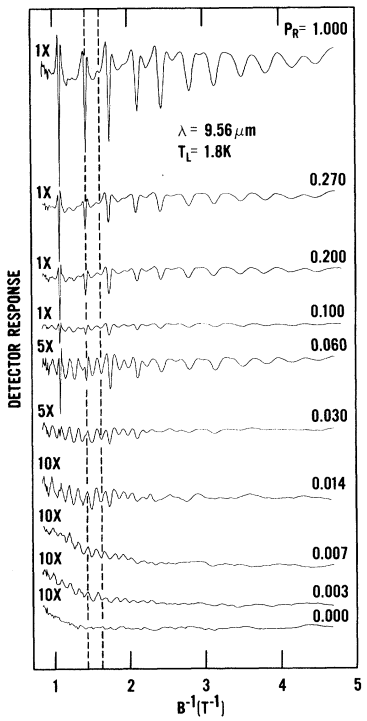

FIG. 1. Photoconductive spectra for different relative peak incident CO_2 laser powers P_R. Note the gain settings on the left. For P_R=1, the peak incident power is ~1.4 W with a beam of 1.5-mm $1/e^2$ intensity diameter. The dashed vertical lines are drawn at the magnetic field positions of a DCRH (high powers) and a LOCRH (lower powers) resonance as discussed in the text and illustrate the fact that the magnetic field positions are independent of laser power.

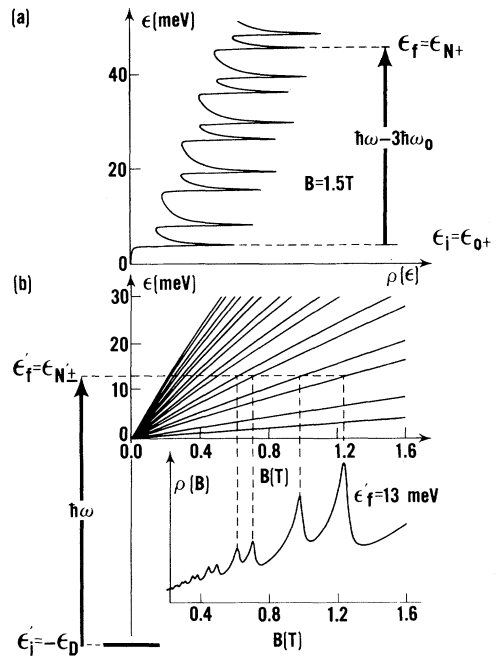

FIG. 2. Schematic representation of the origin of (a) LOCRH and (b) DCRH resonant photoconductive structure as discussed in the text showing the Landau-level variation with magnetic field, the density of states vs energy $\rho(\epsilon)$ and vs magnetic field $\rho(B)$, and the optical transitions involved.

The top trace has a peak incident power of ~1.4 W, while the lower traces were taken with successively smaller values of P_R. The bottom trace was recorded with the laser beam physically blocked. As P_R is increased a series of weak resonant resistivity minima develop. The photoconductive amplitude of this series saturates with increasing laser power, most likely because of depletion of electrons in the initial states. With continued increasing laser power *another* series of very sharply defined resonant resistivity minima develop and at the higher laser powers this structure clearly dominates the photoconductive spectra. Both sets of resonant structures are periodic in inverse magnetic field. The envelope of the resonant structure depends upon the ac field modulation technique.

The origin of the two series of resonant structures in the photoconductivity can be qualitatively understood by a simple Landau-level and density-of-states model schematically represented in Fig. 2. For a fixed magnetic field, the electronic density of states exhibits singularities at the energy corresponding to the bottom of each Landau level. Energy level broadening removes these singularities such that the density of states varies with energy in a manner as shown in Fig. 2(a).

At low powers the resonant structure observed is dominated by three-LO-phonon LOCRH transitions. At resonance, electrons occupy the initial states $\epsilon_i=\epsilon_{0+}$ in the lowest spin-split Landau level and absorb a photon of energy $\hbar\omega$ while emitting three LO phonons of energy $\hbar\omega_0$ to arrive at some final higher Landau level $\epsilon_f=\epsilon_{N+}$. Resonant behavior in the photoconductivity may be observed when the peaks in the density of states are swept through the final-state energy ϵ_f by increasing the field B. Thus, a variation in final density of states with magnetic field is produced and resonant structure arises from an optically created nonequilibrium distribution function with a peak at ϵ_{N+} where the density of states is high. Thus, the mobility and hence conductivity (the number of carriers in the conduction band remains constant) resonantly increase.

At the higher laser powers a different series is observed which we identify as arising from transitions originating from a deep level (at an energy ϵ_D below the conduction-band edge) as shown in Fig. 2(b). The Landau-level energy at $k_z=0$ is shown versus magnetic field B for several Landau levels (N) including spin splitting. Figure 2(b) also shows the variation of the density of states with magnetic field at an energy of 13 meV above the band edge. Consequently, the number of carriers in the conduction band resonantly increases because of the enhanced transition rate resulting from a peak in the final density of states when $\epsilon_f'=\epsilon_{N'\pm}$. In this case the conductivity again resonantly increases at the appropriate magnetic fields.

Figure 3 shows quantitative results on how the resonant structure depends upon photon energy. The observed positions of the minima in resistance (maximum in the conductivity) are plotted as a function of magnetic field for 24 CO_2-laser wavelengths between 9.22 and 10.81 μm. The two series are plotted separately for clarity. Figure 3(a) shows the behavior we attribute to three-phonon LOCRH transitions, while Fig. 3(b) shows the DCRH transitions which we identify as arising from a deep level. In both cases the lines represent our theoretical calculations based upon a Landau-level model of Johnson and Dickey[2] with band parameters of $g=-51.3$ and $E_g=236.7$ meV. For the LOCRH transitions a good fit to the data results with $m_c^*=0.0139m_0$ for the Landau levels and $\hbar\omega_0=24.5$ meV. This is in excellent agree-

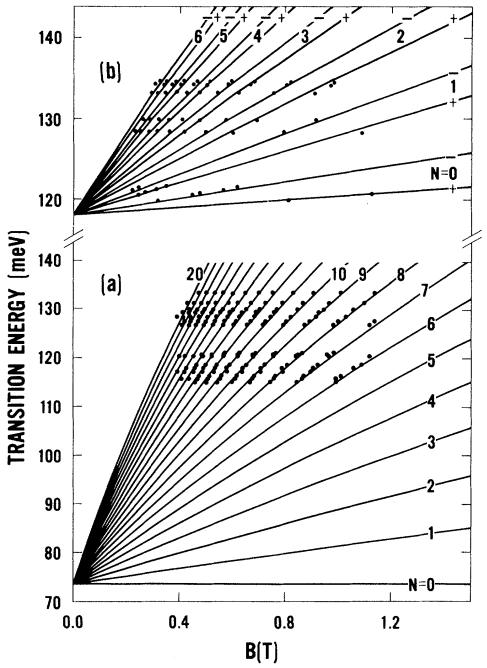

FIG. 3. Transition energies vs magnetic field. The lines are calculated with parameters as discussed in the text.

ment with Johnson and Dickey's results of $0.0139m_0$ and 24.4 meV. Only the lowest spin-split level for each Landau level is plotted since only spin-conserving transitions are observed from the $N=0+$ initial state to final states of $N=6+$ to $20+$.

The spin conservation is consistent with previous results for single-LO-phonon-assisted cyclotron resonance *harmonics*.[2-4] This is because combined-resonance transitions are very weak in comparison to spin-conserving cyclotron resonance[2] and the probability of spin-flip processes induced by optical phonons is low for InSb. On the other hand, electron scattering due to phonons relaxes the selection rules connecting the initial and final states allowing transitions between any two Landau subbands of the same spin. The transition probability for any given initial and final states is given by summing over all possible intermediate (virtual) states and time orderings. Contrary to the single-phonon results,[2,3] we observe resonant structure for both $E \perp H$ and $E \parallel H$ configurations. In our case, for $E \parallel H$, radiative virtual transitions with $\Delta N = 0$ can take place at finite values of k_z while maintaining the resonant condition for initial and final states because of the participation of three LO phonons with negligible dispersion near the zone center.

The fan chart shown in Fig. 3(b) is consistent with DCRH transitions for $\epsilon_i' = \epsilon_D = -118$ meV and $m_c^* = 0.0145m_0$ at wavelengths less than 10.35 μm. Photoconductivity and photoelectromagnetic measurements have indicated a midgap donorlike flaw intrinsic to the InSb lattice.[5,6] Indirect determination of this defect energy by Laff and Fan[5] gave 120 meV above the valence band, in good agreement with the present result. In contrast to the three-phonon processes where spin is conserved, these transitions take place to both spin states and further studies should lead to an enhanced understanding of this defect level.

Is there any other plausible interpretation of the high-power resonant structure than origin from a deep defect level? The initial state of the electron could be (1) the lowest spin-split Landau level or (2) a shallow donor level. If case (1) were true, then the energy intercept at $B=0$ could be attributed to a five-phonon emission process ($5\hbar\omega_0 = 118$ meV, $\hbar\omega_0 = 23.6$ meV). However, the transition rate would involve a sixth order process. Considering the small amplitude of the three-phonon process and the absence of any four-phonon process this hardly seems likely. Most importantly, key features of the data such as the observation of spin-nonconserving transitions and the resonant positions themselves cannot be described by a model of this type!

Optical transitions could originate from shallow donor levels whose energies depend upon magnetic field. One still requires a five-phonon process, which, of course, in a resonant situation may be strong enough to be observed. However, a temperature dependence study of the amplitudes of the high-power structure shows that a finite amplitude exists even out to temperatures of ~95 K. For such high temperatures, very few electrons should be found in shallow donor levels. Consequently, this explanation must also be ruled out. This interpretation is further supported by the temperature dependence of the shift in resonant positions which is consistent with the temperature variation of the band gap.

In summary, we report the first observation of magneto-optical transitions in n-InSb originating from a deep defect level. These transitions along with three-LO-phonon-assisted spin-conserving cyclotron harmonic transitions explain the sharp resonant structure in the CO_2-laser-induced magnetophotoconductivity at low magnetic fields.

Finally, it is interesting to note that the value of m_c^* for the magneto-optical transitions from the mid-gap defect level is consistent with previous interband measurements but conflicts with the intraband result found here and in previous intraband work of others.

The authors gratefully acknowledge the partial support of this research by the U. S. Office of Naval Research and a Faculty Research Grant from North Texas State University.

[1]H. Kahlert and D. G. Seiler, Rev. Sci. Instrum. 48, 1017 (1977).
[2]E. J. Johnson and D. H. Dickey, Phys. Rev. B 1, 2676 (1970).
[3]R. C. Enck, A. S. Saleh, and H. Y. Fan, Phys. Rev. 182, 790 (1969).
[4]R. Grisar, H. Wachering, G. Bauer, J. Wlasak, J. Kowalski, and W. Zawadzki, Phys. Rev. B 18, 4355 (1978).
[5]R. A. Laff and H. Y. Fan, Phys. Rev. 121, 53 (1961).
[6]J. E. L. Hollis, S. C. Choo, and E. L. Heasell, J. Appl. Phys. 38, 1626 (1967).

Theory of Substitutional Deep Traps in Covalent Semiconductors

Harold P. Hjalmarson
Department of Physics and Materials Research Laboratory, University of Illinois at Urbana-Champaign, Urbana, Illinois 61801

and

P. Vogl
Department of Physics and Materials Research Laboratory, University of Illinois at Urbana-Champaign, Urbana, Illinois 61801, and Institut für theoretische Physik,[a] Universität Graz, Graz, Austria

and

D. J. Wolford
IBM Thomas J. Watson Research Center,[a] Yorktown Heights, New York 10598, and Coordinated Science Laboratory and Department of Electrical Engineering, University of Illinois at Urbana-Champaign, Urbana, Illinois 61801

and

John D. Dow
Department of Physics and Materials Research Laboratory,[a] University of Illinois at Urbana-Champaign, Urbana, Illinois 61801, and Solar Energy Research Institute, Golden, Colorado 80401
(Received 5 November 1979)

The energies of substitutional deep A_1 impurity levels in zinc-blende semiconductors are predicted and related to the impurities' atomic energies and to host dangling bond (ideal vacancy) energies.

In this Letter we predict which elements of the periodic table are likely to form substitutional A_1-symmetric traps with energy levels deep within the forbidden band gaps of covalently bonded semiconductors; and we provide a conceptual framework for understanding the major chemical trends in deep-trap energies. This simple but general theory (i) provides a satisfactory definition of what constitutes a "deep" trap[1]; (ii) it explains the major chemical trends in deep-trap energies, including their dependences on the host energy bands and the impurities' atomic structures; (iii) it shows why data for deep-trap energies do not define a single smooth function of impurity atomic energy, even though clear trends with atomic energy are apparent; (iv) it explains why impurities whose atomic energies differ by ~ 10 eV produce trap energies differing by only a fraction of an electron volt[2]; (v) it predicts the derivatives of deep-trap energies with respect to host-alloy composition x in alloys such as $GaAs_{1-x}P_x$ and shows why these derivatives depend only weakly on the impurities[3,4]; and (vi) it explains why in alloys the trap energies do not follow the nearby band edges as x varies, but instead are often nearly linear functions of composition.[3-5]

The central assumption of the present work is that the major chemical *trends* in deep-trap energies are determined by the energy bands of the